NASA Contractor Report 165680

THE PREDICTION OF NORMAL FORCE AND ROLLING MOMENT COEFFICIENTS FOR A SPINNING WING

Barnes W. McCormick

THE PENNSYLVANIA STATE UNIVERSITY
Department of Aerospace Engineering
University Park, Pennsylvania 16802

NASA Purchase Order L-13435B
February 1981

National Aeronautics and
Space Administration

Langley Research Center
Hampton, Virginia 23665

THE PREDICTION OF NORMAL FORCE AND ROLLING MOMENT COEFFICIENTS FOR A SPINNING WING

B. W. McCormick

SUMMARY

The integrated normal force and rolling moment coefficients for a spinning wing are predicted by means of a single strip analysis. Non-linear airfoil section data for angles of attack from 0° to 180° are used in a small computer code to numerically integrate the section normal force coefficients along the span as a function of the local velocity and angle-of-attack resulting from the combined spinning and descending motion. A correction is developed to account for the radial pressure gradient in the separated, rotating flow region above the wing. This correction is found to be necessary in order to obtain agreement, both in form and magnitude, with rotary balance test data.

THE PREDICTION OF NORMAL FORCE AND ROLLING MOMENT COEFFICIENTS FOR A SPINNING WING

B. W. McCormick

INTRODUCTION

The purpose of this study is to predict the normal force and rolling moment coefficients for a spinning wing. These predictions are then compared with experimental measurements obtained with a rotary balance. The predictions are made by calculating the local angles of attack and local dynamic pressures. These determine the wing section normal forces which are then integrated numerically to obtain the normal forces and rolling moment coefficients for the entire wing.

It will be shown that a simple strip analysis, as just described, underestimates the magnitude of the wing's normal force coefficient and also fails, qualitatively, to predict the effect of spin rate on C_N. The strip analysis, of course, neglects 3-D effects caused by induced velocities from the trailing vortex system. However, such effects will generally reduce the C_N prediction and are, thus, not the explanation for the discrepancy between strip analysis and experiment. After some study, it was concluded that the stalled flow above a spinning wing results in centrifugal pumping and, hence, a spanwise pressure gradient, which produces a significant increment in C_N. A relatively simple expression for this increment as a function of spin rate is developed which agrees reasonably well with experiment.

NOMENCLATURE

b	=	wing span, m
c	=	chord, m
C_ℓ	=	rolling moment coefficient
$C_{L_{max}}$	=	maximum wing lift coefficient
C_N	=	normal force coefficient
C_{N_1}	=	parameter in expression for C_N (eq. 4c)
$C_{N_{max}}$	=	parameter in expression for C_N (eq. 4b)
C_{N_α}	=	slope of C_N vs α curve for small α (eq. 4a)
p	=	local static pressure, Pa.
p_c	=	static pressure in separated flow region
q	=	local dynamic pressure, Pa.
v	=	vertical velocity of descent, m/s
x	=	dimensionless spanwise location, $y/(b/2)$
x_s	=	value of x, outboard of which, wing is unstalled
y	=	spanwise distance from wing centerline, m
α	=	section angle of attack, degs
α_L	=	section angle of attack for left wing, degs.
α_R	=	section angle of attack for right wing, degs.
α_2	=	parameter defined in figure 3
α_{max}	=	parameter defined in figure 3
ΔC_ℓ	=	denotes increment in C_ℓ
ΔC_N	=	denotes increment in C_N
ΔN	=	denotes increment in normal force
ε	=	exponent for C_N curve fitting (eq. 4b)

θ = angle between chord line and vertical (fig. 1)

ϕ = angle of chord line from vertical, (eq. 3)

$\bar{\omega}$ = dimensionless spin rate, $\Omega b/2V$

Ω = spin rate, radians/sec.

ANALYSIS

In a steady spin, the right and left wings of an airplane are generally operating at different angles of attack. For a spin to the right, the resultant flow over the right wing may actually be coming from the direction of the trailing edge, which in helicopter rotor terminology is designated as reversed flow.

Consider the sketch given in figure 1 which depicts right and left wing sections in a spin to the right. The figure on the left is a view looking inboard along the left wing and the figure on the right is a similar view for the right wing. The angle of attack of the left wing section, α_L, will be given by,

$$\alpha_L = \theta - \phi \tag{1}$$

and for the right wing,

$$\alpha_R = \pi - \theta - \phi \tag{2}$$

with α_R measured from the trailing edge.

θ is the angle of the chord line from the vertical while the angle ϕ is given by,

$$\phi = \tan^{-1} \frac{\Omega y}{V}$$

Ω being the angular velocity about the spin axis, y the spanwise distance from the centerline and V the descent velocity.

If we let,

$$x = \frac{y}{(b/2)}$$

$$\varpi = \frac{\Omega b}{2V}$$

then ϕ becomes,

$$\phi = \tan^{-1} \bar{\varpi} x \qquad (3)$$

An appreciation for α_L and α_R can be gained from figure 2 which was calculated on the basis of the preceding equations. In this figure, contours of constant α_L and α_R are presented as a function of θ and ϖx. Spotted on the figure are steep and flat spin (or moderately flat) test points for the spin tunnel model and full-scale version of the typical, low-wing general aviation airplane. These points are for the tips with $x = 1.0$. Thus the angles of attack inboard of the tips will be greater than those read from the chart. For the model steep spin, α_L equals approximately 21° and α_R, relative to the leading edge is approximately 50°. The corresponding angles for the full-scale airplane are only 3 to 5° higher. For the flat spin mode however, the angle of attack for the right wing is significantly different between the model and full-scale tests. For the model tests the flow on the right wing tip is reversed at a value of about 60°. On the full-scale airplane, the angle becomes 78° relative to the leading edge.

Since static tests show the model wing to stall at an α of about 10° ($C_{L_{max}} \simeq 1.0$), and even allowing for an increase in $C_{L_{max}}$ with Reynolds number, it would appear that both wings are completely stalled at the test point conditions.

DEVELOPMENT OF PREDICTION METHOD

A small computer program has been developed which performs a strip analysis and numerically integrates along the span to predict a spinning wing normal force coefficient, C_N, and rolling moment coefficient, C_1. The form of the static normal force coefficient vs. α curve used in the program is shown in figure 3,

$$C_N = C_{N_\alpha}\alpha \qquad \alpha \leq \alpha_{max} \qquad (4a)$$

$$C_N = C_{N_{max}}(\sin\alpha)^{\varepsilon} \qquad \alpha \geq \alpha_2 \qquad (4b)$$

$$C_N = C_{N_1} - \left[\frac{\alpha - \alpha_{max}}{\alpha_2 - \alpha_{max}}\right](C_{N_1} - C_{N_2}) \qquad \alpha_{max} \leq \alpha \leq \alpha_2 \qquad (4c)$$

This form for the C_N curve was chosen on the basis of 0012 airfoil and flat plate data. In order to account approximately for 3-D effect, the 0012 data was modified as shown in figure 4. The slope C_{N_α} was corrected for aspect ratio in the usual manner while $C_{N_{max}}$ was reduced on the basis of the variation with aspect ratio of the drag of flat plates normal to the flow. The "section" C_N curve which was finally used is the lower one in figure 4 labeled "3-D wing".

It is interesting to note that the curve is nearly symmetrical about an α of 90^o. Thus an angle of attack relative to the trailing edge will produce the same C_N as that for the same angle relative to the leading edge. Therefore, for θ values near 90^o, where the angle of attack and resultant velocities are nearly equal on the left and right wings, but in opposite directions, one would expect the resultant force on the two sides to be equal. Thus the rolling moment should approach zero, regardless of $\bar{\omega}$, as θ approaches 90^{o}.

In terms of the section C_N values, the wing C_N and C_l can be determined as follows,

$$N = \int_{-b/2}^{b/2} 1/2\rho[V^2 + (\Omega y)^2] C_N C y dy$$

$$\ell = \int_{o}^{b/2} 1/2\rho[V^2 + (\Omega y)^2] C_{N_L} C y \; dy$$

$$- \int_{o}^{b/2} 1/2\rho[V^2 + (\Omega y)^2] C_{N_R} C y \; dy$$

In dimensionless form, for a rectangular wing, these become,

$$C_N = \int_{-1}^{1} \left[1 + (\bar{\omega}x)^2\right] C_N \; dx \tag{5}$$

$$C_\ell = 1/4 \int_{o}^{1} \left[1 + (\bar{\omega}x)^2\right] (C_{N_L} - C_{N_R}) x \; dx \tag{6}$$

The C_N notation is somewhat confusing. Under the integral sign it refers to section data while otherwise, it denotes the normal force coefficient of the entire spinning wing.

INITIAL RESULTS

Equations (5) and (6) were evaluated numerically using figure 4 and eqs. (1) through (4). The results of those calculations are presented in figures 5 and 6 together with rotary balance data. This data was taken from the reference by subtracting fuselage-only data from data for the wing and fuselage combination.

The lack of agreement between predictions and experiment in these figures, particularly for C_N, is obvious. Of most concern is the disagreement in C_N at the higher θ and $\bar{\omega}$ values where flat or moderately flat spins occur. Varying parameters such as C_{N_1}, C_{N_2}, α_{max}, or α_2 within limits did not materially affect the C_N predictions. Increasing $C_{N_{max}}$ merely shifts the curves up in figure 5 without changing the rate of increase of C_N with $\bar{\omega}$ to any appreciable extent. In view of this rate being significantly higher for the data than for the prediction, it was felt that something basic was lacking in the analysis. The usual induced effects were not the answer since downwash corrections would tend to reduce the calculated C_N values even further. Also, compared to a helicopter rotor, the "disc" loading of a spinning airplane is low and its rate of descent high so that its downwash velocities should be low.

After further consideration of this problem, it was realized that the fluid mechanics of the completely-stalled, spinning wing was not being adequately modeled. A correction to C_N which was developed to account for the rotating separated flow will follow.

RADIAL PRESSURE GRADIENT CORRECTION TO C_N

Immediately above a spinning wing, and for some distance beyond, the flow is separated. This means that the fluid in the separated region is moving with the wing in the form of a solid body rotation. Hence, a radial pressure gradient must exist through this fluid given by,

$$\frac{dp}{dr} = \rho r \Omega^2 \tag{7}$$

Integrating, this becomes,

$$p = \frac{\rho (r\Omega)^2}{2} + \text{const.} \tag{8}$$

At r=b/2, p must equal the pressure p_c along the separated streamline at the tip. Thus, using the point to determine the constant in equation (8) results in,

$$p - p_c = - \frac{\rho V^2}{2} \bar{\omega}^2 (1 - x^2) \tag{9}$$

Without the rotation, p_c would be the constant pressure along the back surface of the wing. Hence the pressure decrement, $p - p_c$, results in a increment to C_N calculated purely on the basis of static section normal force coefficients. The increment in the wing's normal force can be written as,

$$\Delta N = 2 \int_0^{b/2} C(p_c - p)\,dy$$

or in coefficient form,

$$\Delta C_N = \int_0^1 \frac{p_c - p}{q}\,dx = \frac{2\bar{\omega}^2}{3} \tag{10}$$

This correction of course only applies to separated flows and is independent of θ provided θ is sufficiently high for a given $\bar{\omega}$, to assure that the wing is stalled.

Referring to figure 2, only the right wing will be completely stalled for a θ of 30^o. Thus, for this case, only half of equation (10) was used in calculating C_N.

Predictions, with and without the correction for the radial pressure gradient are presented in figure 7. The correction is seen to have a significant effect on the shape of the C_N curves, appreciably increasing the C_N values at the higher $\bar{\omega}$ values.

Figure 8 compares the experimental values of C_N with predicted values including the correction for the radial pressure gradient. Here, the agreement is seen to be considerably improved over that of figure 5. On the basis of this figure and the earlier physical reason, it would appear that any calculation of C_N should include the increment given by equation (10).

The radial pressure gradient should not effect the rolling moment, provided both wings are stalled. However, should one wing not be stalled, such as the left wing in a right spin, or vice versa, then a decrement for a right spin or an increment for a left spin should be added to equation (6). Integrating the increment contributed by $p-p_c$ (eq. 9) over one wing and non-dimensionalizing results in,

$$\Delta C_\ell = \pm\bar{\omega}^2/16 \tag{11}$$

For a right spin this correction is negative. For the values of θ shown here, the left wing is installed over at least the outer 70% of its span for a θ of 30°. At 50° there may be a slight correction. Thus the correction given by (11) was applied to the calculated C_l values only for $\theta = 30^\circ$ and is included in figure 6.

As a refinement, the corrections to C_N and C_l can be derived for the more general case where the advancing wing (left wing in a right spin) is unstalled outboard of a station X_s. This is done by integrating eq. (8) only out to X_s and setting p equal to p_c at that location. In this case equations (10) and (11) become,

$$\Delta C_N = \frac{\bar{\omega}^2}{3}(1 + X_s^3) \tag{12}$$

$$\Delta C_\ell = \frac{\bar{\omega}^2}{16}(1 - X_s^2)^2 \tag{13}$$

The program appended to this report includes these corrections. The program checks to see if any portion of the wing is unstalled and sets X_s accordingly.

CONCLUSIONS

An approximate method has been developed for predicting normal force and rolling moment coefficients for a spinning wing. Fair agreement is obtained with experimentally-measured coefficients but only if a correction is included to account for the radial pressure gradient produced above the wing by the rotating separated flow.

REFERENCE

William Bihrle, Jr., Randy A. Hultberg, and William Mulcay, Rotary Balance Data for a Typical Single-Engine Low-Wing General Aviation Design for an Angle-of-Attack Range of 30° to 90°, NASA CR 2972, July 1978.

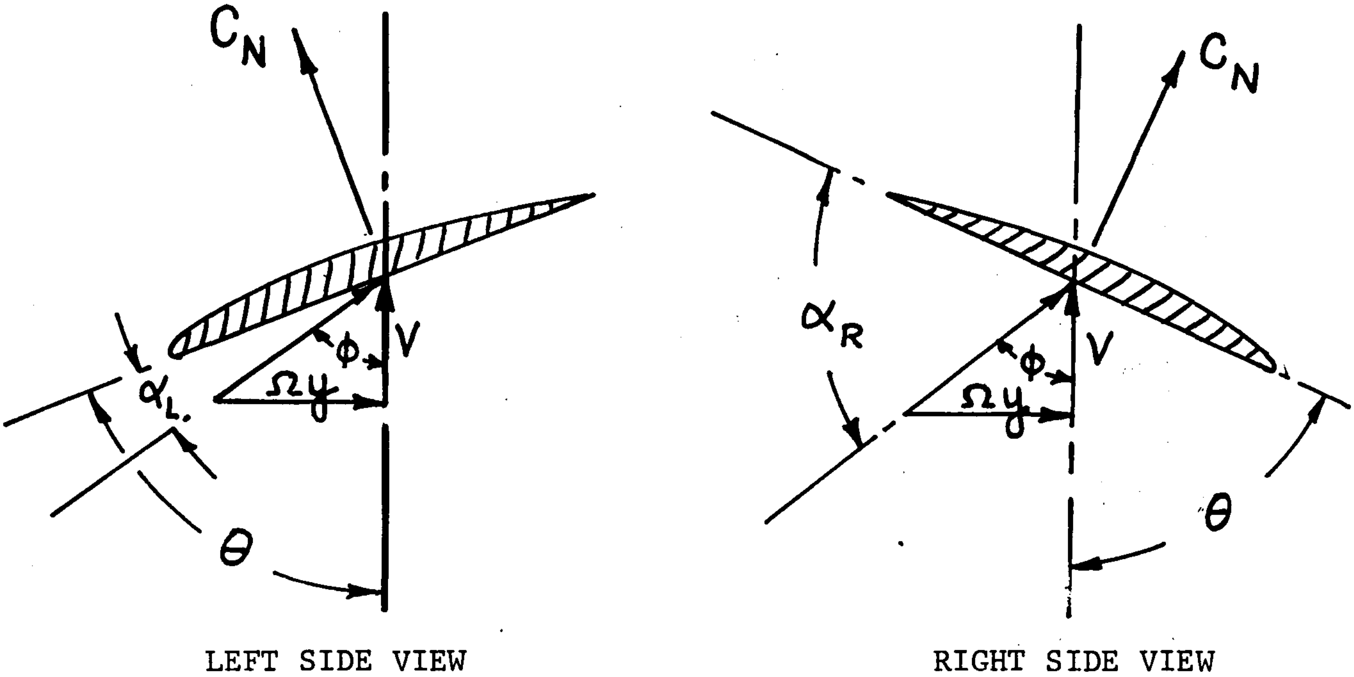

FIGURE 1

Velocities Influencing Left and Right
Sections of a Wing in a Right Spin

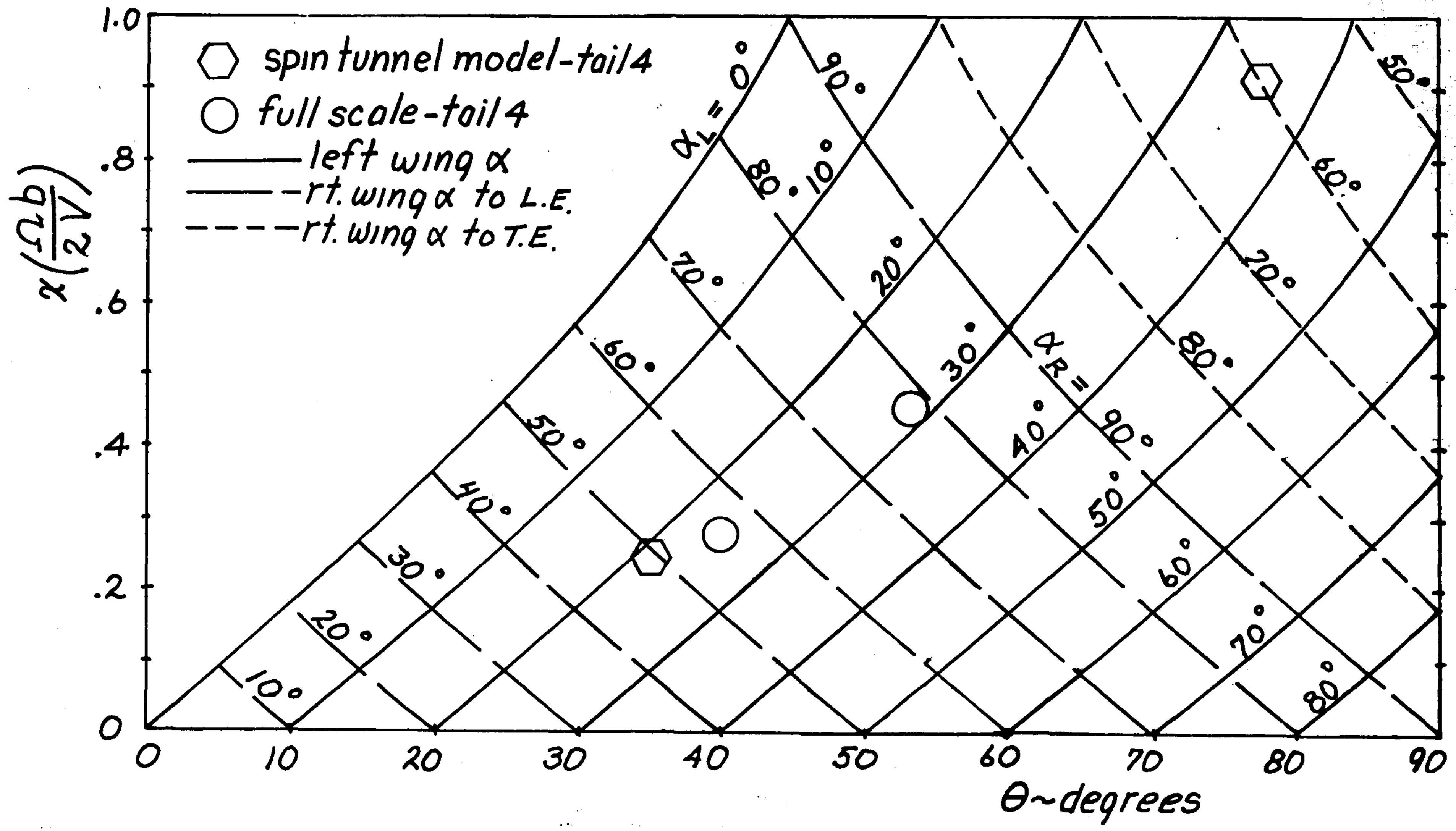

FIGURE 2

Local Angles of Attack on Left and Right Wings for a Right Spin. (Test points for Wing tips x = 1)

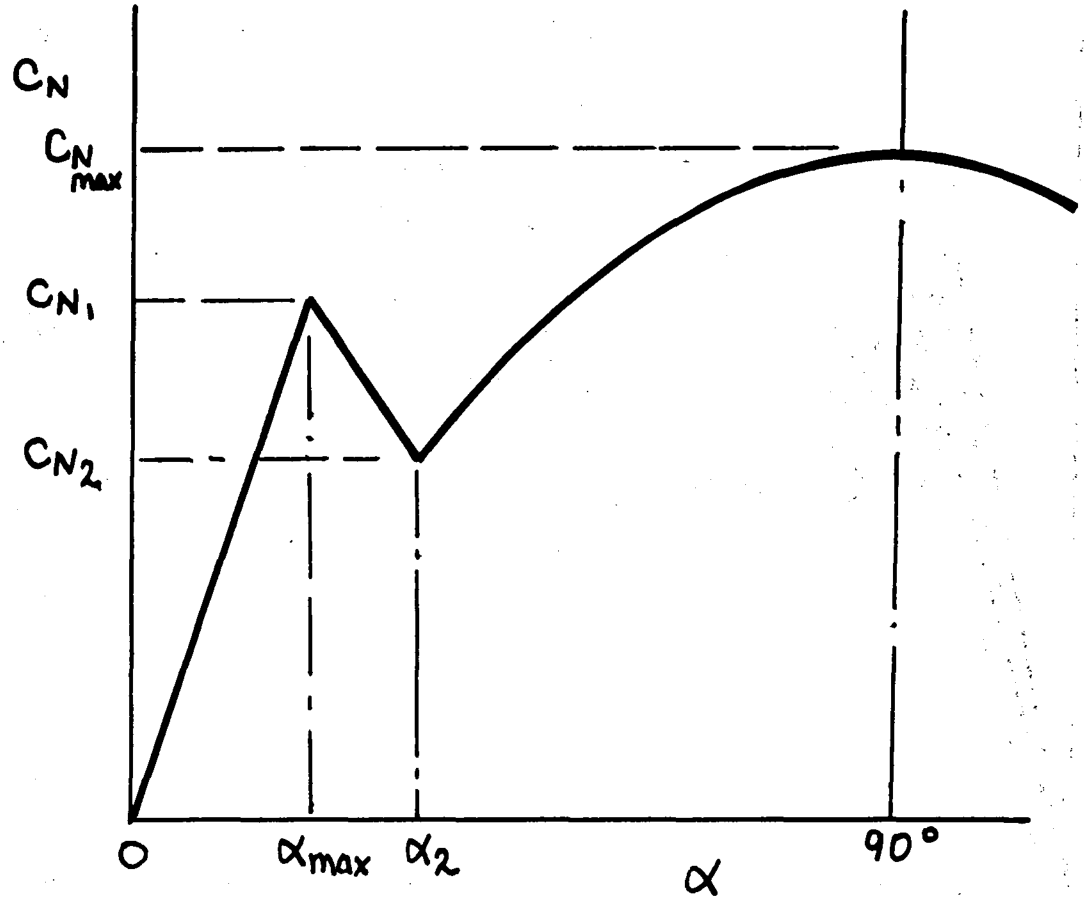

FIGURE 3

Model of C_N Curve
for Airfoil Section

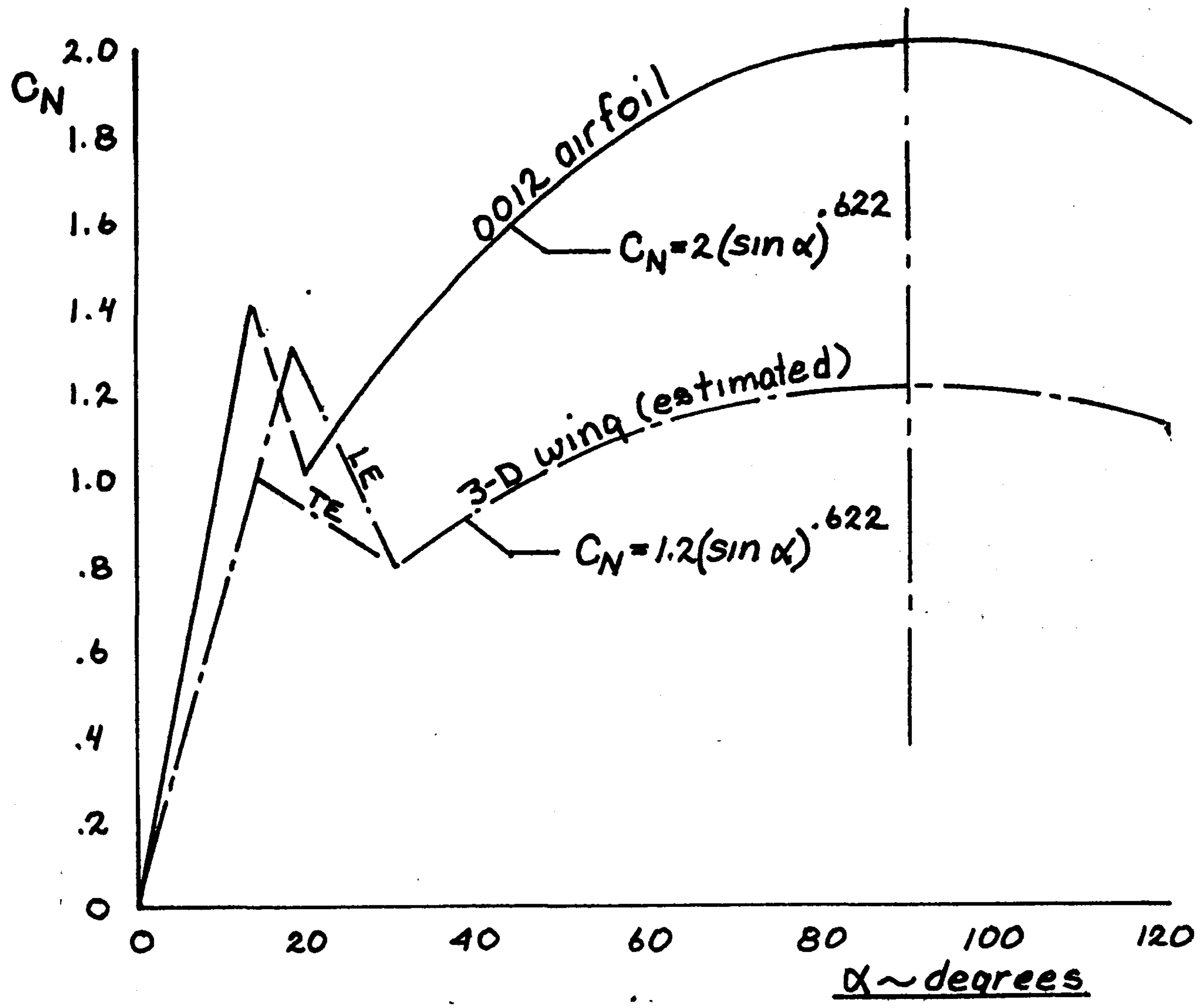

FIGURE 4

Airfoil and Wing Normal
Force Coefficients
(static)

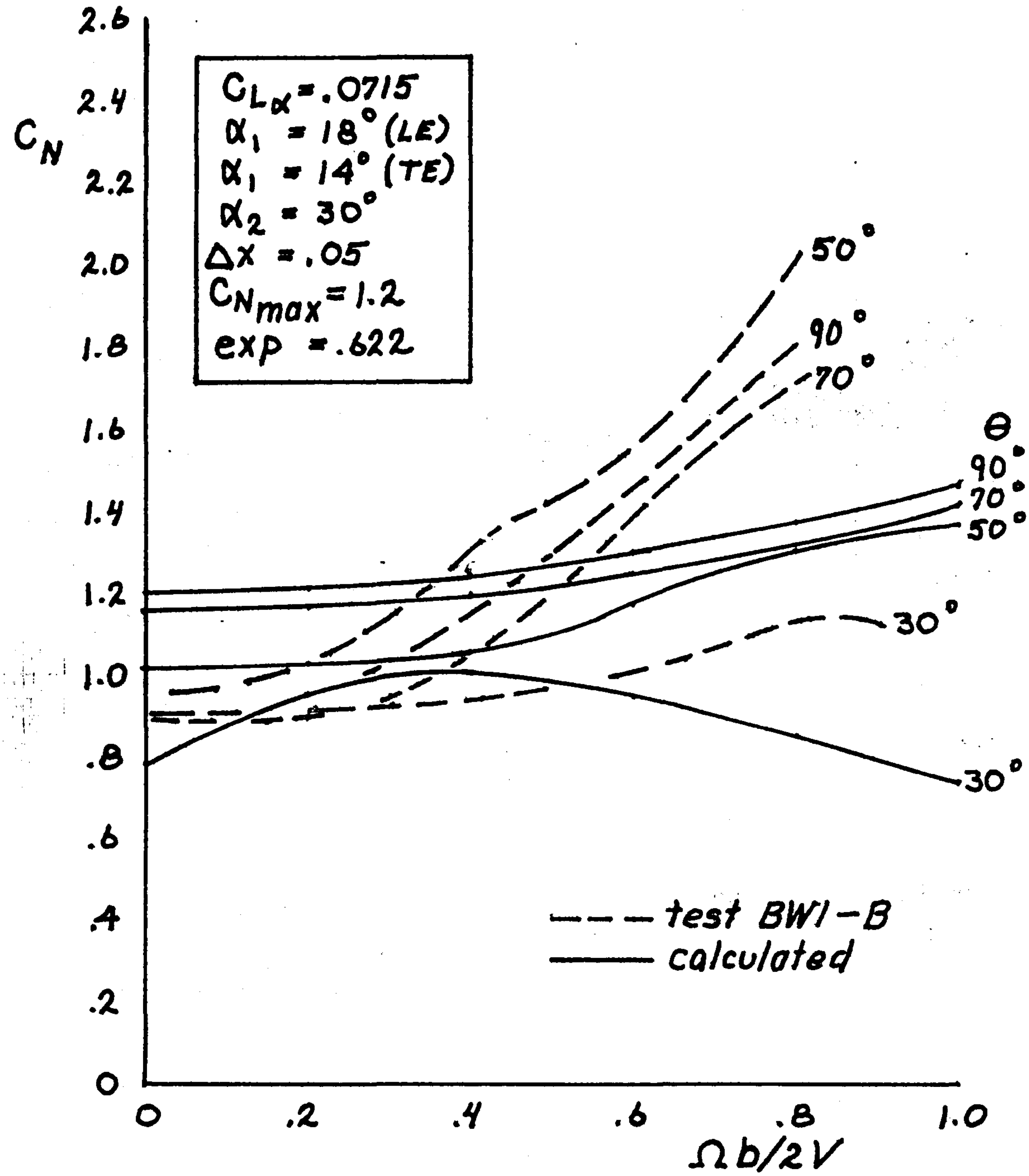

FIGURE 5

Calculated and Measured Normal
Force Coefficients for a Spinning Wing

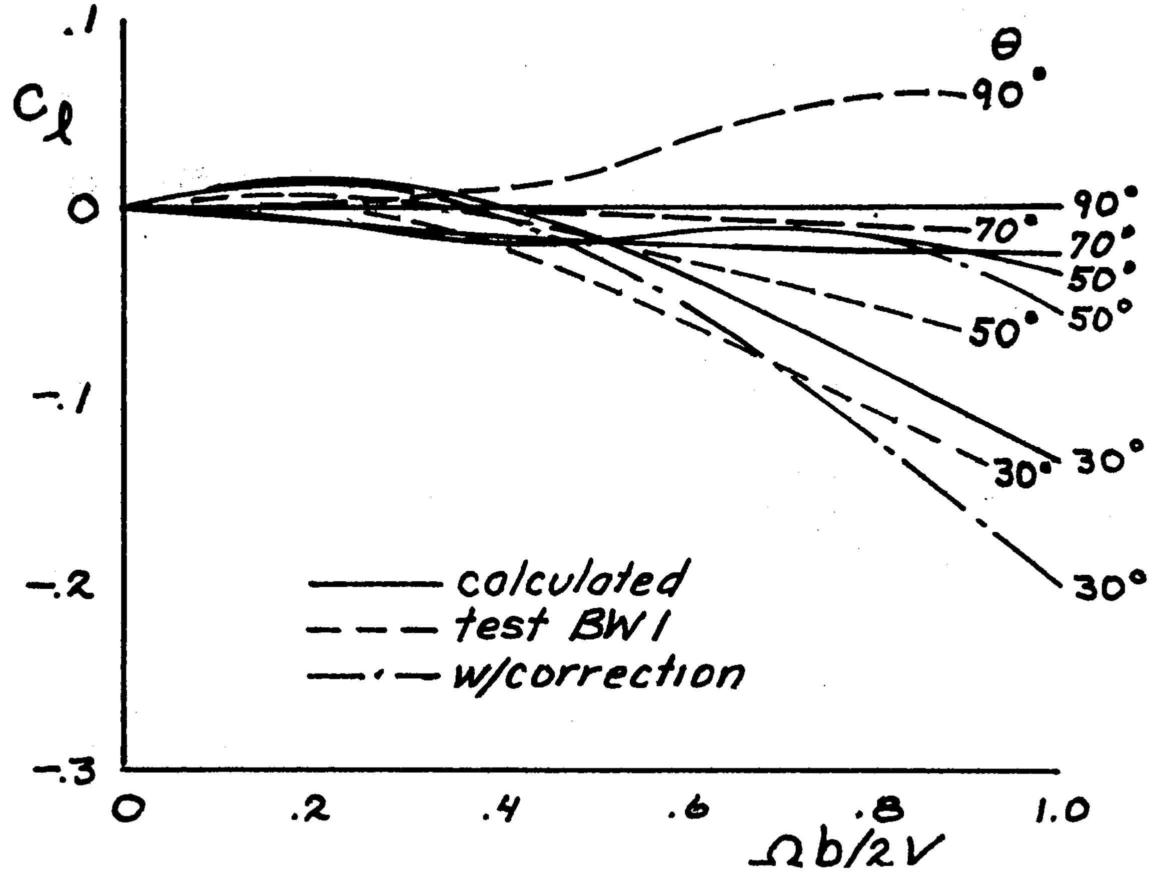

FIGURE 6

Predicted and Measured Rolling Moment
Coefficients for a Spinning Wing

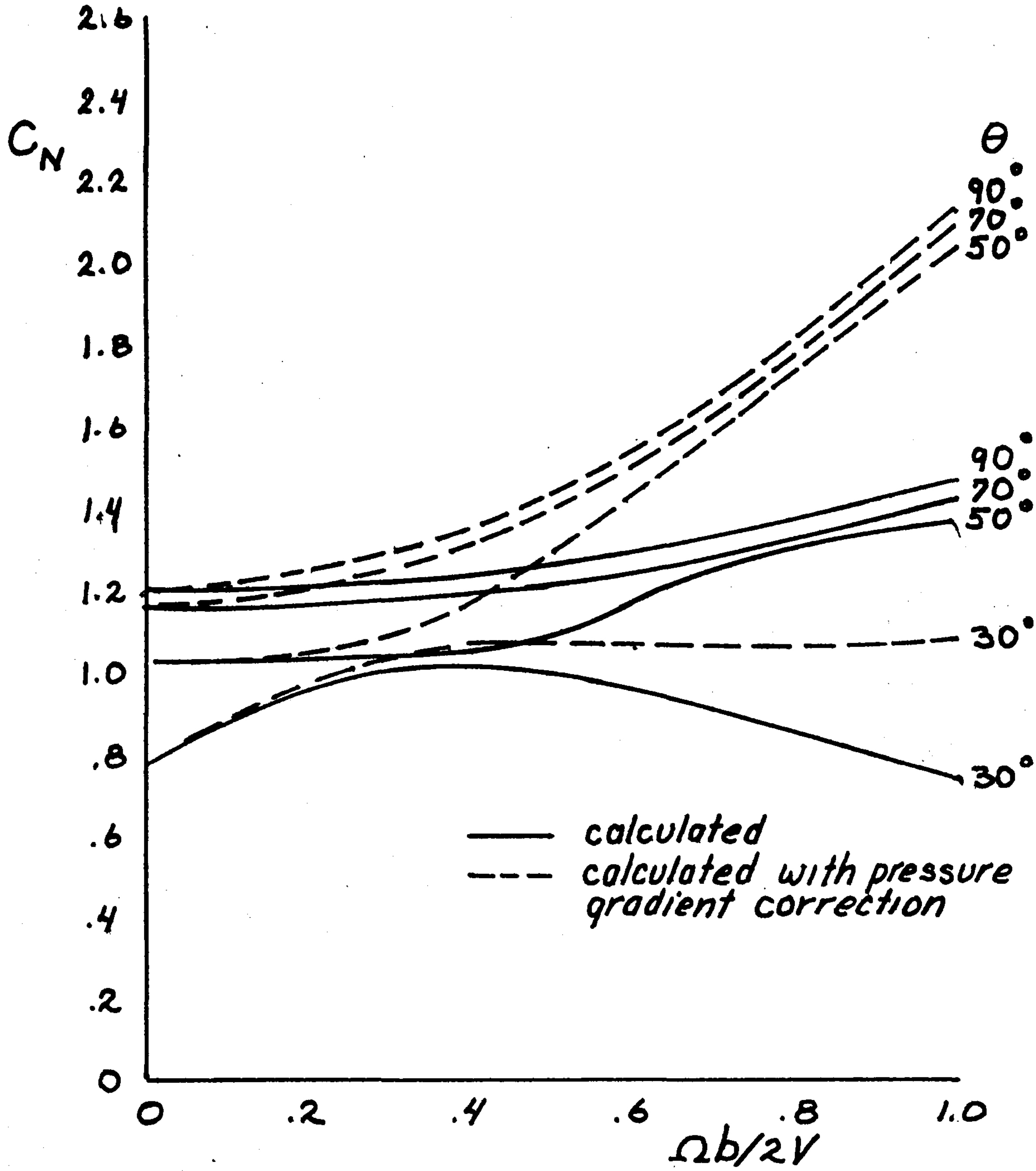

FIGURE 7

Effect of Radial Pressure Gradient on
Predicted Normal Force Coefficients for
a Spinning Wing

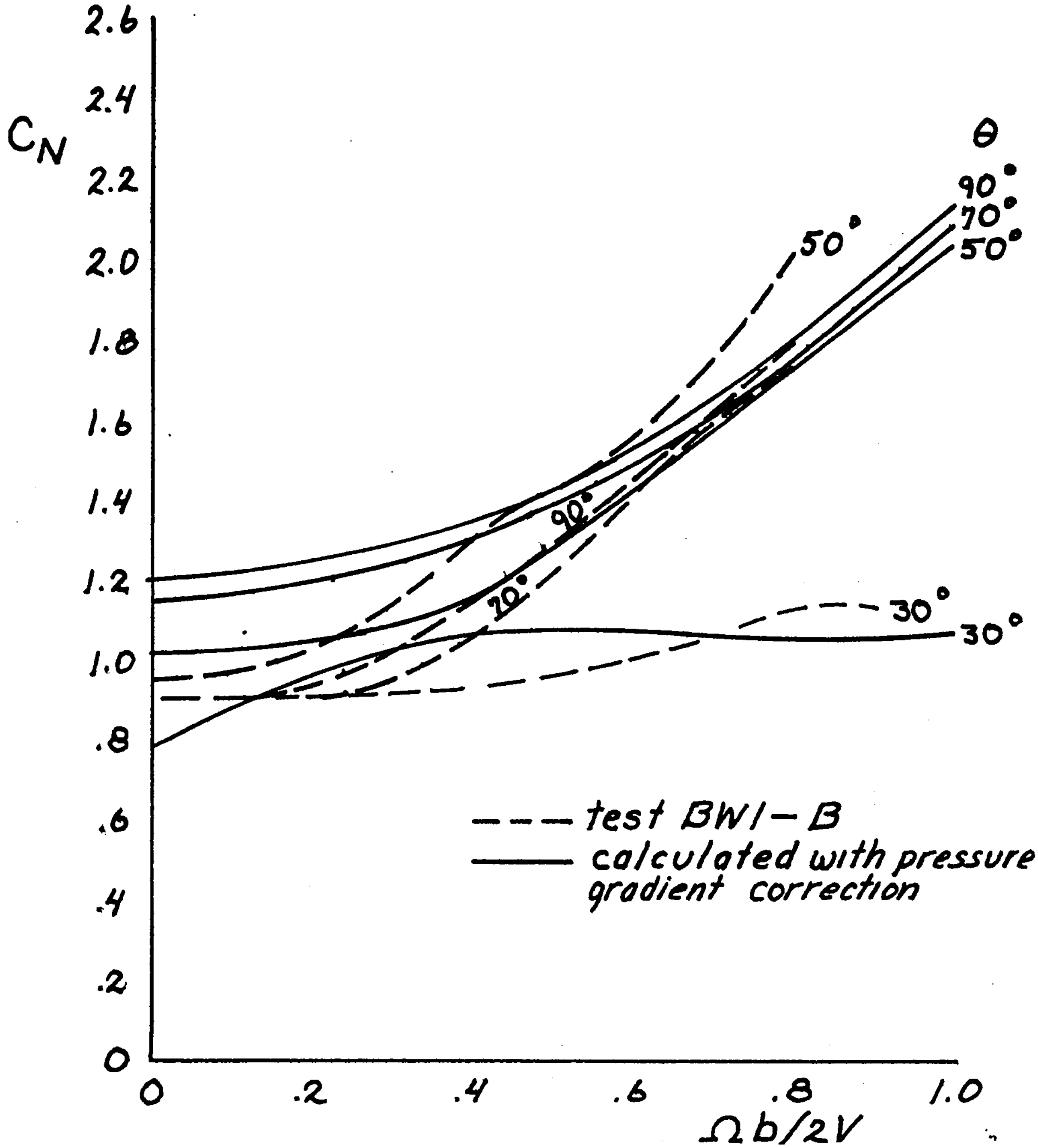

FIGURE 8

Comparison with Experiment of Predicted Normal Force Coefficients for a Spinning Wing including Radial Pressure Gradient

APPENDIX

```
      PROGRAM CNCL3D(INPUT,OUTPUT,TAPE5=INPUT,TAPE6=OUTPUT)
C     THIS PROGRAM PERFORMS A STRIP ANALYSIS TO CALCULATE NORMAL FORCE
C     AND ROLLING MOMENT COEFFICIENTS ON A WING.
C     CNW=WING NORMAL FORCE COEFFICIENT
C     CLW=WING ROLLING MOMENT COEFFICIENT
C     CNWC=WING NORMAL FORCE COEFFICIENT CORRECTED FOR RADIAL GRADIENT
C     CLWC=WING ROLLING MOMENT COEFFICIENT CORRECTED FOR RADIAL GRADIENT
C     LIFT CURVE INCREASES LINEARLY UP TO ANGLE ALLE (FOR LEADING EDGE)
C     OF ALTE (FOR TRAILING EDGE). IT THEN DECREASES LINEARLY TO AN
C     ANGLE AL2 WHICH IS ON THE COMPLETELY STALLED CURVE.  ALONG THIS
C     PORTION OF THE LIFT CURVE CN IS APPROXIMATED BY THE RELATIONSHIP
C     USED IN THE PROGRAM TWO LINES BEFORE STATEMENT 2.
C     FOR A GIVEN INPUT, CALCULATIONS BEGIN AT AN ANGLE OF ATTACK OF
C     30 DEGREES AND GO UP TO 90 DEGREES.  AT EACH ANGLE COMPUTATIONS
C     ARE PERFORMED OVER A RANGE OF DIMENSIONLESS SPIN RATES FROM 0 TO 1
C     DELX = INCREMENT INSPANWISE DISTANCE FOR NUMERICAL INTEGRATION
C     EXPRESSED AS A FRACTION OF THE SEMI-SPAN. ALL ANGLES AND LIFT
C     CURVE SLOPE , CLA, ARE PUT IN IN DEGREES. TYPICAL INPUT VALUES ARE
C     CLA=0.072  ALLE=16.0   ALTE=14.0   AL2=30.   DELX=.05   CNMAX=1.2
C     EXPCN=.622   THESE ARE 2-D VALUES AND SHOULD BE USED FOR THE
C     STRIP ANALYSIS.  THE PROGRAM HAS NO 3-D CORRECTIONS.
C     THETA IS RELATIVE TO WING ZERO LIFT LINE
      READ(5,100)CLA,ALLE,ALTE,AL2,DELX,CNMAX,EXPCN
      CHAY=-1.
      AL2=AL2/57.3
      ALLE=ALLE/57.3
      ALTE=ALTE/57.3
      CLA=CLA*57.3
      CN1LE=ALLE*CLA
      CN1TE=ALTE*CLA
      CN2=CNMAX*(SIN(AL2))**EXPCN
      CNW=0.
      CLW=0.
      OMEGA=0.
      THETA=30.
      THETA=THETA/57.3
      X=-1.
    1 CONTINUE
      PHI=ATAN(OMEGA*ABS(X))
      ALPHAL=THETA-PHI
      ALPHAR=3.14159-THETA-PHI
      VRSOD=1.+(OMEGA*X)**2
      IF(X.GT.0.)GO TO 2
      ALPHA=ALPHAL
      IF(ALPHA.LT.ALLE)CN=CLA*ALPHA
      IF(ALPHA.LT.ALLE)XS=X
      IF(ALPHA.LT.ALLE)CHAY=1.
      IF(ALPHA.LT.ALLE)GO TO 3
      IF(ALPHA.LT.AL2)CN=CN1LE-(ALPHA-ALLE)/(AL2-ALLE)*(CN1LE-CN2)
      IF(ALPHA.LT.AL2)GO TO 3
      CN=CNMAX*(SIN(ALPHA))**EXPCN
      GO TO 3
```

APPENDIX

```
    2 CONTINUE
      ALPHA=ALPHAR
      IF(ALPHA.LT.ALTE)CN=CLA*ALPHA
      IF(ALPHA.LT.ALTE)GO TO 3
      IF(ALPHA.LT.AL2)CN=CN1TE-(ALPHA-ALTE)/(AL2-ALTE)*(CN1TE-CN2)
      IF(ALPHA.LT.AL2)GO TO 3
      CN=CNMAX*(SIN(ALPHA))**EXPCN
    3 CONTINUE
      DCNW=.5*VRSQD*CN
      DCLW=-DCNW*X/4.
      IF(X.EQ.-1.)GO TO 4
      CNW=CNW+(DCNW+DCNW1)/2.*DELX
      CLW=CLW+(DCLW+DCLW1)/2.*DELX
      DCNW1=DCNW
      DCLW1=DCLW
      X=X+DELX
      IF(X.GT.1.)GO TO 5
      GO TO 1
    4 DCNW1=DCNW
      DCLW1=DCLW
      X=X+DELX
      GO TO 1
    5 CONTINUE
      THETA=THETA*57.3
      IF(CHAY.EQ.-1.)XS=1.0
      CNWC=CNW+OMEGA**2/3.*(1.+XS**3)
      CLWC=CLW-OMEGA**2/16.*(1.-XS**2)**2
      WRITE(6,101)OMEGA,THETA,CNW,CLW,CNWC,CLWC
      OMEGA=OMEGA+.2
      CNW=0.
      CLW=0.
      X=-1.
      THETA=THETA/57.3
      IF(OMEGA.GT.1.)GO TO 6
      GO TO 1
    6 CONTINUE
      OMEGA=0.
      THETA=THETA+10./57.3
      IF(THETA.GT.90./57.3)GO TO 7
      GO TO 1
    7 CONTINUE
      CLA=CLA/57.3
      ALLE=ALLE*57.3
      ALTE=ALTE*57.3
      AL2=AL2*57.3
      WRITE(6,102)CLA,ALLE,ALTE,AL2,DELX,CNMAX,EXPCN
      STOP
  100 FORMAT(7F10.4)
  101 FORMAT(2X,6HOMEGA=,F5.2,4X,6HTHETA=,F6.2,4X,3HCN=,F7.3,4X,3HCL=,F7
     1.3,4X,5HCNWC=,F7.3,4X,5HCLWC=,F6.4)
  102 FORMAT(2X,4HCLA=,F7.4,4X,5HALLE=,F7.2,4X,5HALTE=,F7.2,4X,4HAL2=,F7
     1.2,4X,5HDELX=,F7.4,4X,6HCNMAX=,F7.2,4X,6HEXPCN=,F7.3)
      END
```

1. Report No.	2. Government Accession No.	3. Recipient's Catalog No.
NASA CR-165680		

4. Title and Subtitle	5. Report Date
The Prediction of Normal Force and Rolling Moment Coefficients For A Spinning Wing	February 1981
	6. Performing Organization Code
7. Author(s)	8. Performing Organization Report No.
Barnes W. McCormick	
	10. Work Unit No. 505-41-13-06
9. Performing Organization Name and Address The Pennsylvania State University Department of Aerospace Engineering 233 Hammond Building University Park, PA 16802	11. Contract or Grant No. L-13435B
12. Sponsoring Agency Name and Address National Aeronautics and Space Administration Washington, DC 20546	13. Type of Report and Period Covered Contractor Report
	14. Sponsoring Agency Code

15. Supplementary Notes

Langley Technical Monitor: Daniel J. DiCarlo
Topical Report

16. Abstract

The integrated normal force and rolling moment coefficients for a spinning wing are predicted by means of a single strip analysis. Non-linear airfoil section data for angles of attack from 0^o to 180^o are used in a small computer code to numerically integrate the section normal force coefficients along the span as a function of the local velocity and angle of attack resulting from the combined spinning and descending motion. A correction is developed to account for the radial pressure gradient in the separated, rotating flow region above the wing. This correction is found to be necessary in order to obtain agreement, both in form and magnitude, with rotary balance test data.

17. Key Words (Suggested by Author(s))	18. Distribution Statement
Wing Aerodynamics Analytical Prediction Spinning General Aviation High Angle of Attack Data Rotary Balance Data	Unclassified - Unlimited Subject Category 05

19. Security Classif. (of this report)	20. Security Classif. (of this page)	21. No. of Pages	22. Price*
Unclassified	Unclassified	21	A02

N-305

End of Document